Deuteron production in a combined thermal and coalescence framework for heavy-ion collisions in the few-GeV energy regime

Wojciech Florkowski

Institute of Theoretical Physics, Jagiellonian University

March 15, 2024

WF, Piotr Salabura, Nikodem Witkowski and Radosław Ryblewski

Acta Phys. Pol. B55 (2024) 2-A2

Short introduction

Recently formulated statistical hadronization model of hadron production in heavy-ion collisions in the few-GeV energy regime allowed to describe transverse mass and rapidity spectra of hadrons.

Main point of this model is assumption of *spherical* (Phys. Rev. C, 102(5):054903, 2020) or *spheroidal* (Phys. Rev. C, 107(3):034917, 2023) expansion instead of classical formalism of boost-invariant blast-wave models used in high-energy regime.

In this work, we continue the analysis of the data collected by the HADES Collaboration for Au-Au collisions at the beam energy $\sqrt{s_{\mathrm{NN}}} = 2.4$ GeV and the centrality class of 10%.

Fits to the particles abundances suggest two different sets of possible freeze-out thermodynamic parameters. The main difference between them resides in two different values of the freeze-out temperature: $T = 49.6$ MeV vs. $T = 70.3$ MeV, reffered as low- and high-temperature ones.

In total we discuss 3 models: low-temperature spherical model, and low- and high-temperature spheroidal models called "A" and "B" respectively.

Thermodynamic parameters

Three versions of the model

Parameter	Spherical	Spheroidal A	Spheroidal B
T (MeV)	49.6	49.6	70.3
μ_B (MeV)	776	776	876
μ_{I_3} (MeV)	−14.1	−14.1	−21.5
R (fm)	16.02	15.7	6.06
H (MeV)	8.0	10.0	22.5
δ	0	0.2	0.4
$v_R = \tanh(HR)$	0.57	0.66	0.60
$\gamma_R = \cosh(HR)$	1.22	1.33	1.25

Geometry

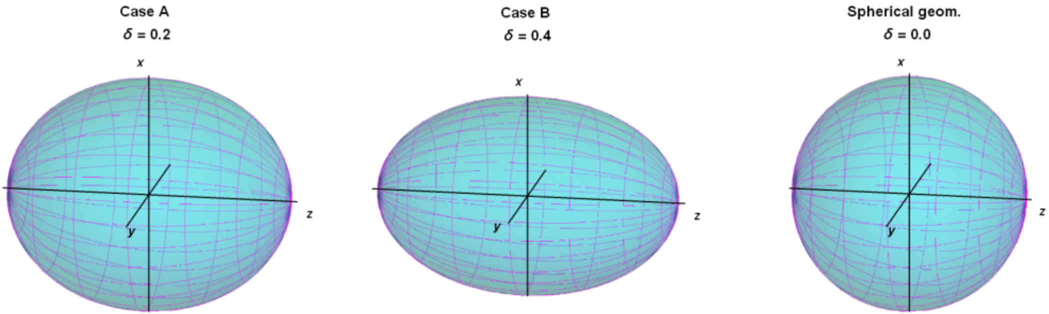

Figure: Graphical representation of the flow parametrization for the three studied cases. The points on the surfaces represent solutions of the equation $(v_x^2 + v_y^2)/(1-\delta) + v_z^2/(1+\delta) = v^2$.

Coalescence model

The basic idea of the coalescence model for deuteron production is that the deuteron spectrum is obtained as the product of proton and neutron spectra taken at half of the deuteron momentum.

$$F_p(\boldsymbol{p}) = \frac{dN_p}{d^3p}, \quad F_n(\boldsymbol{p}) = \frac{dN_n}{d^3p}, \tag{1}$$

and the deuteron distribution as the product:

$$\frac{dN_d}{d^3p_d} = A_{\mathrm{FR}}\, F_p\left(\frac{\boldsymbol{p}_d}{2}\right) F_n\left(\frac{\boldsymbol{p}_d}{2}\right), \tag{2}$$

where A_{FR} is the deuteron formation rate coefficient, while the subscripts d, p, n refer to deuterons, protons, and neutrons, respectively.

As in both theory and experiment one usually deals with invariant momentum distributions, $E\,dN/(d^3p)$ it is useful to recall that for cylindrically symmetric (with respect the beam axis z) we have:

$$\frac{dN}{d^3p} = \frac{dN}{2\pi\,E\,dy\,p_\perp dp_\perp} = \frac{dN}{2\pi E\,dy\,m_\perp dm_\perp}, \tag{3}$$

where E is the on-mass-shell energy of a particle $E = \sqrt{m^2 + \boldsymbol{p}^2}$ and $m_\perp$ is its transverse mass $m_\perp = \sqrt{m^2 + p_\perp^2}$. Therefore, from (2) we obtain:

$$\frac{dN_d}{E_d\,dy\,m_{\perp d} dm_{\perp d}} = \frac{A_{\mathrm{FR}}}{2\pi} \frac{dN_p}{E\,dy\,m_\perp dm_\perp} \frac{dN_n}{E\,dy\,m_\perp dm_\perp}. \tag{4}$$

For finite values of rapidity

$$\frac{dN_d}{dy\,m_{\perp d}^2 dm_{\perp d}} = \frac{A_{\mathrm{FR}}}{2\pi\cosh y} \frac{dN_p}{dy\,m_\perp^2\,dm_\perp} \frac{dN_n}{dy\,m_\perp^2\,dm_\perp}. \tag{5}$$

A popular form of the coefficient A_{FR} used in the literature is Acta Phys. Polon. B, 48:707, 2017 (Mrówczyński):

$$A_{\mathrm{FR}} = \frac{3}{4}(2\pi)^3 \int d^3r\, D(r)\, |\phi_d(r)|^2 . \tag{6}$$

Here the function $D(r)$ is the normalized to unity distribution of the relative space positions of the neutron and proton pairs at freeze-out, while $\phi_d(r)$ is the deuteron wave function

The most popular choice for those two functions are Gaussian profiles:

$$D(r) = \left(4\pi R_{\mathrm{kin}}^2\right)^{-3/2} \exp\left(-\frac{r^2}{4R_{\mathrm{kin}}^2}\right), \tag{7}$$

$$|\phi_d(r)|^2 = \left(4\pi R_d^2\right)^{-3/2} \exp\left(-\frac{r^2}{4R_d^2}\right), \tag{8}$$

where R_{kin} is the radius of the system at freeze-out and $R_d = 2.13$ fm is the deuteron radius.

Expression (7) gives the root-mean-squared value $r_{\rm rms} = \sqrt{6}R \approx 2.45R$, which implies deuteron production far away from the original thermal system and its long formation time
Thus, as an alternative to the Gaussian distribution (7), we use the distribution of a relative distance for particles produced independently in a sphere of radius R, later sharp-cutoff model:

$$D(r) = \frac{3}{4\pi R^3}\left(1 - \frac{3r}{4R} + \frac{r^3}{16R^3}\right)\theta_H(2R - r). \tag{9}$$

Also for the deuteron wave function we use the Hulthen wave function defined by the expression Phys. Rev. C, 103(1):014907, 2021

$$\phi_d(r) = \sqrt{\frac{\alpha\beta(\alpha+\beta)}{2\pi(\alpha-\beta)^2}}\,\frac{\exp(-\alpha r) - \exp(-\beta r)}{r}, \tag{10}$$

where $\alpha = 0.2\ \mathrm{fm}^{-1}$ and $\beta = 1.56\ \mathrm{fm}^{-1}$.[1] Both $D(r)$ and $|\phi_d(r)|^2$ are normalized to unity.

[1] We use here traditional notation, β appearing in (10) should not be confused with inverse temperature.

Distribution profiles

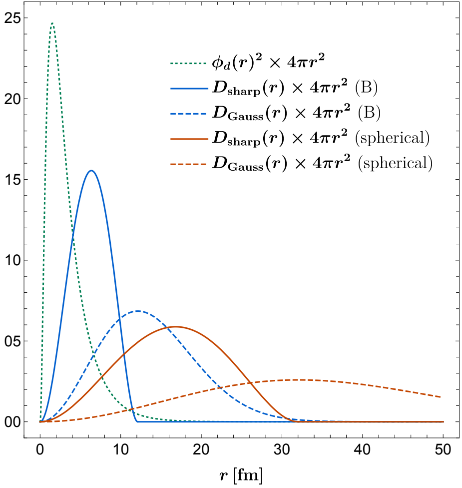

Figure: The square of the Hulthen wave function and different versions of the nucleon pair distribution function $D(r)$ multiplied by the factor $4\pi r^2$.

Formation ratio values

Formation rate	Spherical	A	B
A_{GG} (MeV^3)	7 565	8 028	120 509
A_{SG} (MeV^3)	64 239	67 860	693 463
A_{SH} (MeV^3)	69 661	73 735	942 476

Table: Values of the formation rate parameter A_{FR} for different choices of the functions $D(r)$ and $\phi_d(r)$: A_{GG} is obtained with the two Gaussian profiles, Eqs. (7) and (8), and $R_{\mathrm{kin}} = R$; A_{SG} follows from Eqs. (9) and (8); finally, A_{SH} is calculated with Eqs. (9) and (10).

We observe that the values of A_{FR} do not significantly differ for the spherical and spheroidal A cases – they are both low-temperature scenarios with large freeze-out radii. However, an increase in the magnitude of A_{FR} is clearly seen if we switch from the Gaussian to the sharp cutoff distribution of pairs. An additional increase of the magnitude of A_{FR} is seen if we switch to the spheroidal B scenario. In this case, the freeze-out radius is relatively small (~ 6 fm) and the overlap of the pair distribution with the deuteron wave function becomes the largest.

Cooper-Frye formula

The standard starting point for quantitative calculations is the Cooper-Frye formula that describes the invariant momentum spectrum of particles:

$$E\frac{dN}{d^3p} = \int d^3\Sigma_\mu(x)\, p^\mu f(x,p). \qquad (11)$$

Here $f(x,p)$ is the phase-space distribution function of particles, and $p^\mu = (E, \boldsymbol{p})$ is their four-momentum with the mass-shell energy $E = \sqrt{m^2 + \boldsymbol{p}^2}$.
The infinitesimal element of a three-dimensional freeze-out hypersurface from which particles are emitted $d^3\Sigma_\mu(x)$ may be obtained from the formula:

$$d^3\Sigma_\mu = -\epsilon_{\mu\alpha\beta\gamma}\frac{\partial x^\alpha}{\partial a}\frac{\partial x^\beta}{\partial b}\frac{\partial x^\gamma}{\partial c}\, da\, db\, dc, \qquad (12)$$

where $\epsilon_{\mu\alpha\beta\gamma}$ is the Levi-Civita tensor with the convention $\epsilon_{0123} = -1$ and a, b, c are the three independent coordinates introduced to parametrize the hypersurface. This allows us to construct a six-dimensional, Lorentz invariant density of the produced particles:

$$d^6N = \frac{d^3p}{E}\, d^3\Sigma \cdot p\; f(x,p). \qquad (13)$$

The independent variables in such a general parametrization would be three components of three-momentum and the variables a, b, and c.

Phase-space distribution function

Assuming local equilibrium the phase-space distribution function have general form:

$$f(x,p) = f(u \cdot p) = \frac{g_s}{(2\pi)^3}\left[\Upsilon^{-1}\exp\left(\frac{u \cdot p}{T}\right) - \chi\right]^{-1}, \tag{14}$$

where $\chi = -1$ ($\chi = +1$) for Fermi-Dirac (Bose-Einstein) statistics, $g_s = 2s + 1$ is spin degeneracy, T is temperature of system and Υ is fugacity factor.
In models fugacity factor takes form:

$$\begin{aligned} \Upsilon_p &= \exp\left(\frac{\mu_B + \frac{1}{2}\mu_{I_3}}{T}\right), \\ \Upsilon_n &= \exp\left(\frac{\mu_B - \frac{1}{2}\mu_{I_3}}{T}\right). \end{aligned} \tag{15}$$

where μ_B and μ_{I_3} are baryon and isospin chemical potentials, respectively.

Spherical Symmetry

Spherical Symmetry

Parametrization

First model assumes spherical symmetry of fireball and single-freeze-out approach was used to define freeze-out hypersurface. Expansion of fireball is treated as Hubble like with constant H to avoid non-zero speed of the centrum of the fireball. This assumptions and usage of spherical coordinates, leads to the following parametrization:

$$d^3\Sigma_\mu = (1,0,0,0)r^2 \sin\theta d\theta d\phi dr, \tag{16}$$

$$u^\mu = \gamma(r)\,(1, v(r)\boldsymbol{e}_r) \tag{17}$$

with $\boldsymbol{e}_r = (\cos\phi\sin\theta, \sin\phi\sin\theta, \cos\theta)$,

$$p^\mu = (E, p\,\boldsymbol{e}_p)\,, \tag{18}$$

with $\boldsymbol{e}_p = (\cos\phi_p\sin\theta_p, \sin\phi_p\sin\theta_p, \cos\theta_p)$.

$$v(r) = \tanh(Hr), \tag{19}$$

Sphericall symmetry allows to calculate needed expressions in the phase-space distribution, namely:

$$u \cdot p = \gamma(r)\left(E_p - pv(r)\kappa\right), \tag{20}$$

$$d^3\Sigma \cdot p = E_p r^2 \sin\theta d\theta d\phi dr, \tag{21}$$

$$\gamma(r) = \cosh(Hr). \tag{22}$$

where $\kappa \equiv \boldsymbol{e}_p \cdot \boldsymbol{e}_r = \cos\theta\cos\theta_p + \sin\theta\sin\theta_p\cos(\phi - \phi_p)$.

Proton distribution function

Using parametrization from slide before, and Fermi-Dirac distribution, one can obtain proton distribution function in form:

$$\frac{dN}{dym_\perp^2\,dm_\perp} = \frac{g_s\cosh y}{(2\pi)^2}\int\limits_0^R dr\,r^2\int\limits_0^\pi d\theta\sin\theta\int\limits_0^{2\pi} d\phi \times\left[\Upsilon^{-1}\exp\left(\frac{\gamma(r)(E-p\,v(r)\kappa)}{T}\right)+1\right]^{-1}. \quad (23)$$

Due to spherical symmetry, the integral on the RHS of (23) is independent of the angles θ_p and ϕ_p, hence we may set $\theta_p = \phi_p = 0$ ($\kappa = \cos\theta$) and write:

$$\frac{dN}{dy\,m_\perp^2\,dm_\perp} = \cosh y\ S(p) \quad (24)$$

where:

$$S(p) = \frac{g_s}{2\pi}\int\limits_0^R dr\,r^2\int\limits_0^\pi d\theta\sin\theta \times\left[\Upsilon^{-1}\exp\left(\frac{E\cosh(Hr)-p\,\sinh(Hr)\cos\theta}{T}\right)+1\right]^{-1}. \quad (25)$$

Protons in spherical model

In the spherical case, our results for protons and neutrons depend only on the magnitude of their three-momentum:

$$p = \sqrt{p_x^2 + p_y^2 + p_z^2} = \sqrt{p_\perp^2 + m_\perp^2 \sinh^2 y}. \tag{26}$$

Hence, the transverse-momentum distribution of protons or neutrons at zero rapidity is directly given by the function $S(p_\perp)$, namely:

$$\left.\frac{dN_{p,n}}{dy\, m_\perp^2\, dm_\perp}\right|_{y=0} = S_{p,n}(p_\perp). \tag{27}$$

On the other hand, the rapidity distribution is given by the integral:

$$\frac{dN}{dy} = \cosh y \int\limits_m^\infty S\left(\sqrt{p_\perp^2 + m_\perp^2 \sinh^2 y}\right) m_\perp^2 dm_\perp. \tag{28}$$

Results

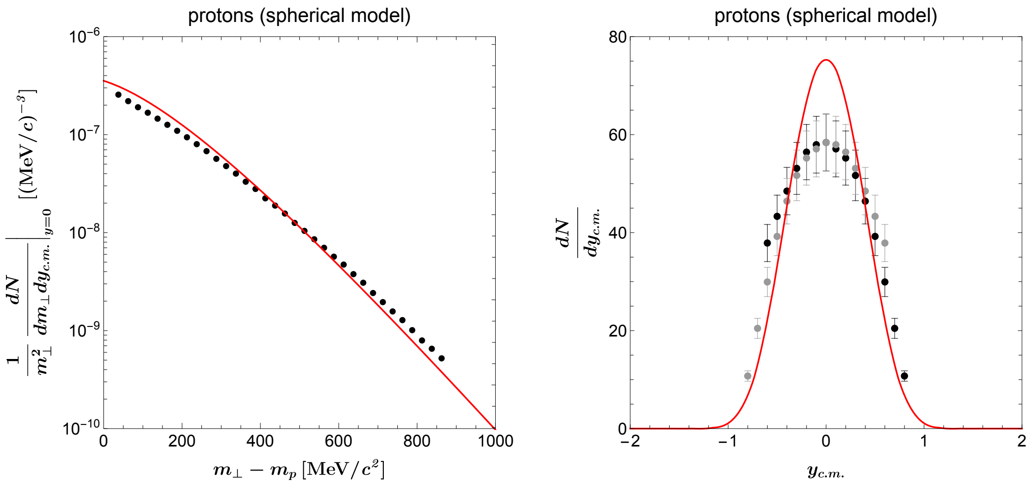

Figure: Transverse-momentum (**left**) and rapidity (**right**) spectra of protons obtained in the spherical model (solid red lines) compared with the HADES data. The experimental errors of the transverse-momentum spectra are within the data points. Brighter points in the right panel are mirror ($y \to -y$) reflections. The total yield of protons N_p is 72.0, while the experimental result is 77.6, hence differs by less than 10%.

Having the proton model spectra reproduced, we can turn to the analysis of the deuteron production. In this case, we use (27), and rewrite (4) in a compact form as:

$$\left.\frac{dN_d}{dy\, m_{\perp d}^2 dm_{\perp d}}\right|_{y=0} = \frac{A_{\mathrm{FR}}}{2\pi} S_p \left(\frac{p_{\perp d}}{2}\right) S_n \left(\frac{p_{\perp d}}{2}\right), \tag{29}$$

where we can use the substitution $p_{\perp d} = \sqrt{m_{\perp d}^2 - m_d^2}$. For finite values of rapidity, we use:

$$\begin{aligned} \frac{dN_d}{dy\, m_{\perp d}^2 dm_{\perp d}} &= \frac{A_{\mathrm{FR}}}{2\pi \cosh y} S_p \left(\frac{\sqrt{m_{\perp d}^2 \cosh^2 y - m_d^2}}{2}\right) \\ &\times S_n \left(\frac{\sqrt{m_{\perp d}^2 \cosh^2 y - m_d^2}}{2}\right). \end{aligned} \tag{30}$$

Results

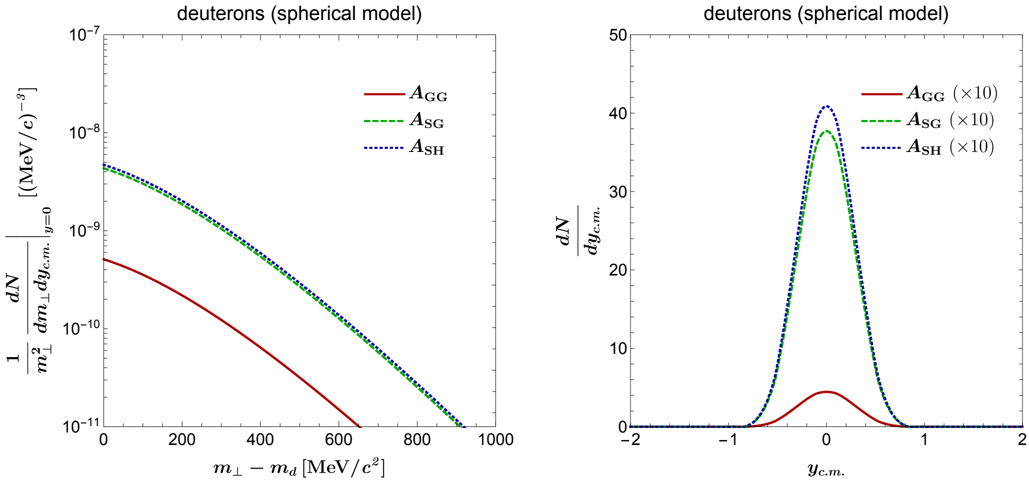

Figure: Predictions of the spherical model for the deuteron production. **Left:** model transverse-momentum spectra obtained for three different values of the formation rate coefficient A_{FR} (as given in Table 1). **Right:** model rapidity distributions. The biggest obtained yield is $N_d \approx 2.88$, while the measured deuteron yield is 28.7.

Spheroidal model

Parametrization

For spheroidally symmetric freeze-outs with respect to the beam axis, it is convenient to introduce the following parametrization of the space-time points on the freeze-out hypersurface:

$$x^\mu = \left(t, r\sqrt{1-\epsilon}\,\boldsymbol{e}_{r\perp}, r\sqrt{1+\epsilon}\,\cos\theta\right). \tag{31}$$

Here the parameter ϵ controls deformation from a spherical shape, while $\boldsymbol{e}_{r\perp} = (\cos\phi\sin\theta, \sin\phi\sin\theta)$. For $\epsilon > 0$ the hypersurface is stretched in the (beam) z-direction.The resulting infinitesimal element of the spheroidally symmetric hypersurface has the form:

$$d^3\Sigma_\mu = (1-\epsilon)(\sqrt{1+\epsilon}, 0, 0, 0) r^2 \sin\theta d\theta d\phi dr, \tag{32}$$

$$u^\mu = \gamma(r,\theta)\left(1, v(r)\sqrt{1-\delta}\boldsymbol{e}_{r\perp}, v(r)\sqrt{1+\delta}\cos\theta\right), \tag{33}$$

$$p^\mu = (E_p, p\boldsymbol{e}_p), \tag{34}$$

$$v(r) = \tanh(Hr), \tag{35}$$

Those relations allows to write needed expressions in the phase-space distribution as:

$$u \cdot p = \gamma(r,\theta)\left[E_p - pv(r)\kappa(\delta)\right], \tag{36}$$

where $\kappa(\delta) = \sqrt{1+\delta}\cos\theta\cos\theta_p + \sqrt{1-\delta}\sin\theta\sin\theta_p\cos(\phi-\phi_p)$,

$$d^3\Sigma \cdot p = (1-\epsilon)\sqrt{1+\epsilon}E_p r^2 \sin\theta d\theta d\phi dr, \tag{37}$$

$$\gamma(r,\theta) = \left[1-(1+\delta\cos(2\theta))v(r)^2\right]^{-\frac{1}{2}}. \tag{38}$$

earlier analysis of the spectra showed that a very good description of the data can be obtained by assuming single freeze-out and $\epsilon = 0$, however with $\delta \neq 0$. Then, we have, as in the spherical case:

$$d^3\Sigma \cdot p = E\, r^2 dr \sin\theta\, d\theta\, d\phi. \tag{39}$$

The Cooper-Frye formula for fermions takes the form:

$$\frac{dN}{dy\, m_\perp^2\, dm_\perp} \quad = \quad \cosh y\; \tilde{S}(p, \theta_p) \tag{40}$$

where :

$$\tilde{S}(p, \theta_p) \quad = \quad \frac{g_s}{(2\pi)^2} \int_0^R dr\, r^2 \int_0^\pi d\theta \sin\theta \int_0^{2\pi} d\phi \left[\Upsilon^{-1} \exp\left(\frac{u \cdot p}{T}\right) + 1\right]^{-1}. \tag{41}$$

With $u \cdot p$ given by (36), where due to the spheroidal symmetry we can set $\phi_p = 0$.

Finally, by changing variables from p and θ_p to rapidity and transverse mass, we may write:

$$\frac{dN}{dy\, m_\perp^2\, dm_\perp} \quad = \quad \cosh y\ \tilde{S}\left[\sqrt{m_\perp^2 \cosh^2 y - m^2}, \theta_y(m_\perp, y)\right], \tag{42}$$

where:

$$\theta_y(m_\perp, y) = \arccos \frac{m_\perp \sinh y}{\sqrt{m_\perp^2 \cosh^2 y - m^2}}. \tag{43}$$

We note that within our approximations the angle (43) is the same for nucleons and deuterons. At zero rapidity we obtain as the special case:

$$\left.\frac{dN}{dy\, m_\perp^2\, dm_\perp}\right|_{y=0} \quad = \quad \tilde{S}\left(p_\perp, \frac{\pi}{2}\right). \tag{44}$$

Results

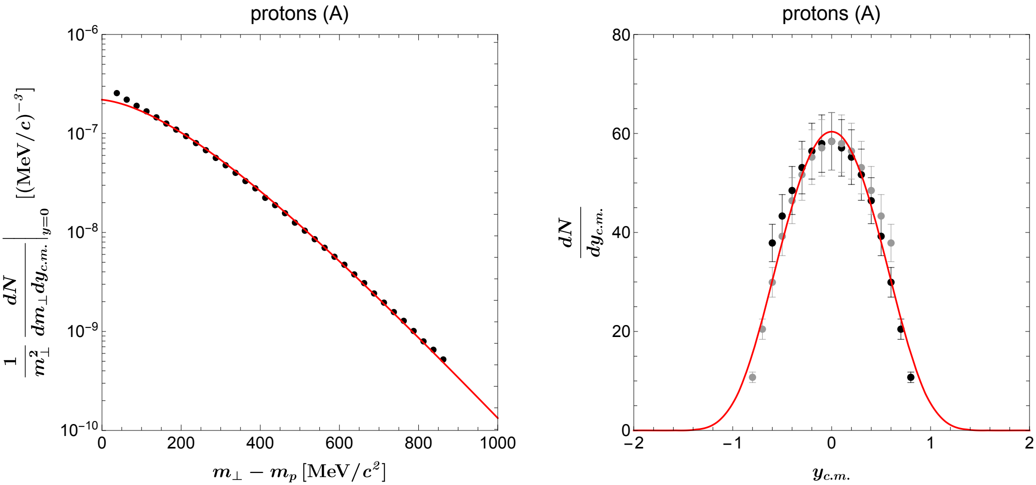

Figure: Transverse-momentum (**left**) and rapidity (**right**) spectra of protons obtained in the spherical model version A (solid red lines) compared with the HADES data. The experimental errors of the transverse-momentum spectra are within the data points. Brighter points in the right panel are mirror ($y \to -y$) reflections. The total yield of protons N_p is 73.78, while the experimental result is 77.6, hence differs by less than 5%.

Results

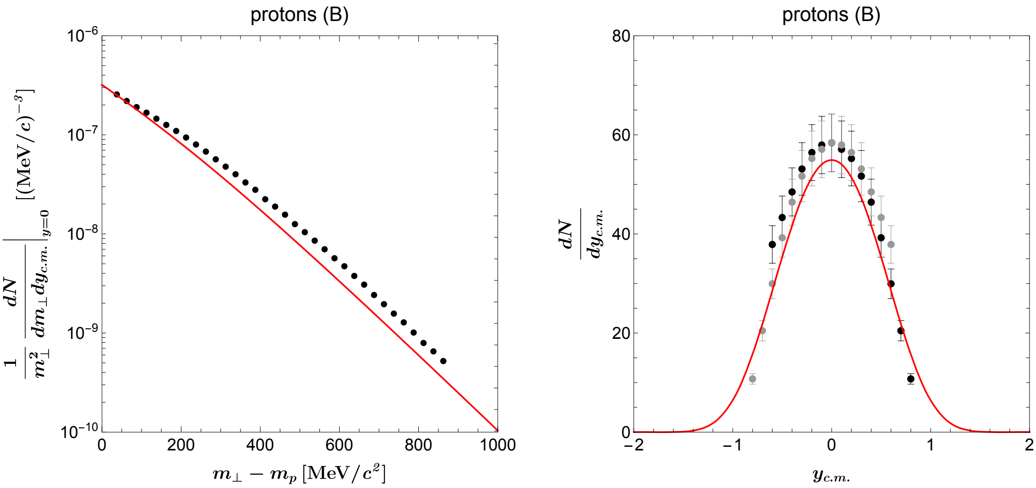

Figure: Same as Fig. 5 but for the spheroidal model version B. The total yield of protons N_p is 69.35, while the experimental result is 77.6, hence differs by $\approx 10\%$. The contribution from the Delta resonance is not included here (the complete result with Delta is shown in Phys. Rev. C, 107(3):034917, 2023 [?].

Having checked that we can reproduce the proton spectra, we can make predictions for the deuterons. In this case, we use (30) with the nucleon spectrum defined by Eq. (42). Our numerical results are presented in Table 2.

Deuterons in spheroidal model A

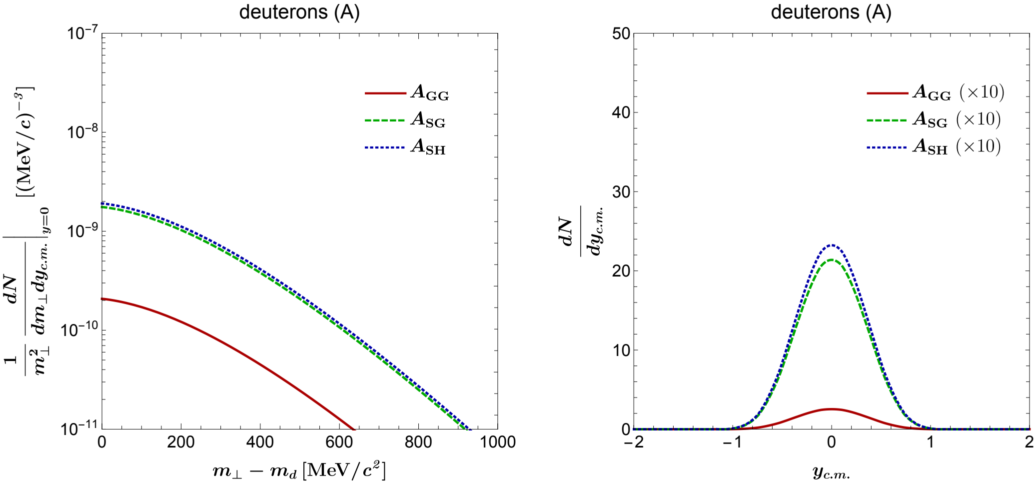

Figure: Predictions for the deuteron spectra in the spheroidal model version A. The biggest obtained yield is $N_d \approx 2.02$, while the measured deuteron yield is 28.7.

Deuterons in spheroidal model B

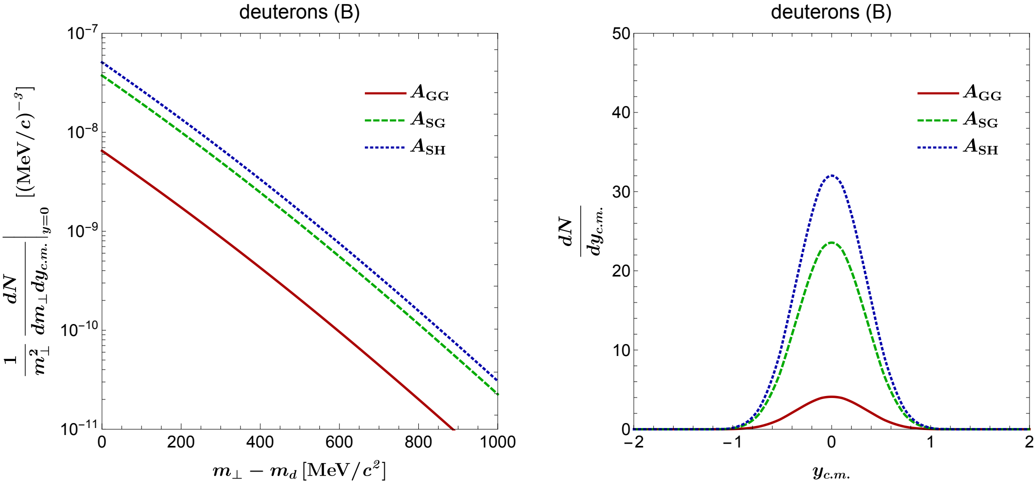

Figure: Predictions for the deuteron spectra in the spheroidal model version B. The biggest obtained yield is $N_d \approx 27.04$, while the measured deuteron yield is 28.7, hence differs by $\approx 5\%$.

Results

Model A	A_{GG}	A_{SG}	A_{SH}
N_d	0.22	1.86	2.02
$(dN_d/dy)_{y=0}$	0.25	2.14	2.32
Model B	**A_{GG}**	**A_{SG}**	**A_{SH}**
N_d	3.46	19.89	27.04
$(dN_d/dy)_{y=0}$	4.09	23.56	32.02

Table: Model results for N_d and $(dN_d/dy)_{y=0}$ obtained for the spheroidal model A (the second and third lines) and the spheroidal model B (the fourth and fifth line). The second, third, and fourth columns correspond to different values of the formation rate coefficient A.

Total yield of deuterons in high-temperature spheroidal model is $N_d \approx 27.04$, while the measured deuteron yield is 28.7, hence differs by $\approx 5\%$.

Conclusions

Conclusions

Conclusions

We find that the slope of the transverse-momentum spectra of deuterons follows naturally from the main coalescence ansatz that the deuteron spectrum is the product of nucleon spectra taken at half of the deuteron three-momentum. However, the normalization of the deuteron spectrum depends very strongly on the value of the so-called formation rate coefficient.

Both, a higher freeze-out temperature (a smaller system's size) and a non-Gaussian distribution of the distance between the original pairs forming the deuteron increase the probability that a nucleon pair forms a deuteron. Each of these effects increases the formation rate by a factor of 10.

At the level of the proton and pion spectra (the latter are not shown here), the three considered herein freeze-out models give very similar quantitative descriptions of the data — the standard deviations for the spheroidal models A and B are $Q = 0.238$ and $Q = 0.256$ (Phys. Rev. C, 107(3):034917, 2023), respectively. Taking into account the measured yield of deuterons, our present work favors, however, the freeze-out scenario at a higher freeze-out temperature combined with a spheroidal expansion. This case may be further examined by a study of other interesting aspects such as the contribution from the Delta resonance, Lambda spin polarization (as in Phys. Rev. C 100(5):054907, 2019), and the production of other light nuclei.